
DiTTo-TTS: Efficient and Scalable Zero-Shot Text-to-Speech with Diffusion Transformer

Keon Lee
KRAFTON
keonlee@krafton.com

Dong Won Kim
KRAFTON
dwkim@krafton.com

Jaehyeon Kim
KRAFTON
jay.310@krafton.com

Jaewoong Cho
KRAFTON
jwcho@krafton.com

Abstract

Large-scale diffusion models have shown outstanding generative abilities across multiple modalities including images, videos, and audio. However, text-to-speech (TTS) systems typically involve domain-specific modeling factors (e.g., phonemes and phoneme-level durations) to ensure precise temporal alignments between text and speech, which hinders the efficiency and scalability of diffusion models for TTS. In this work, we present an efficient and scalable Diffusion Transformer (DiT) that utilizes off-the-shelf pre-trained text and speech encoders. Our approach addresses the challenge of text-speech alignment via cross-attention mechanisms with the prediction of the total length of speech representations. To achieve this, we enhance the DiT architecture to suit TTS and improve the alignment by incorporating semantic guidance into the latent space of speech. We scale the training dataset and the model size to 82K hours and 790M parameters, respectively. Our extensive experiments demonstrate that the large-scale diffusion model for TTS without domain-specific modeling not only simplifies the training pipeline but also yields superior or comparable zero-shot performance to state-of-the-art TTS models in terms of naturalness, intelligibility, and speaker similarity. Our speech samples are available at <https://ditto-tts.github.io>.

1 Introduction

Large-scale diffusion models have demonstrated impressive generative abilities in a wide range of fields including images [1, 2], videos [3, 4], and audio [5, 6]. The integration of latent diffusion models (LDMs) [7] further amplifies their popularity [8, 9, 10], as these models significantly enhance computational efficiency. This efficiency is achieved through the reduction of input dimensionality using autoencoders, which also enables the diffusion models to focus on the most critical features of data [7]. However, applying LDMs to text-to-speech (TTS) presents unique challenges because TTS requires precise alignment between text and generated speech over time. Hence, their application to TTS often requires a complex pipeline, incorporating speech domain-specific modeling such as phoneme and duration [11, 12]. Without these components, generation performance tends to be suboptimal [13, 14], while their inclusion hinders the model efficiency and scalability.

In this work, we present a latent diffusion model for TTS that is integrated with off-the-shelf pre-trained text and speech encoders without relying on the speech domain-specific modeling. Our method addresses the challenge of aligning text and speech solely through cross-attention mechanisms. Furthermore, we introduce a module that predicts the total duration of the generated speech from a given text and speech prompt, rather than determining the duration of each individual input token. To accomplish this, we conduct a network architecture ablation to identify a model specifically suited

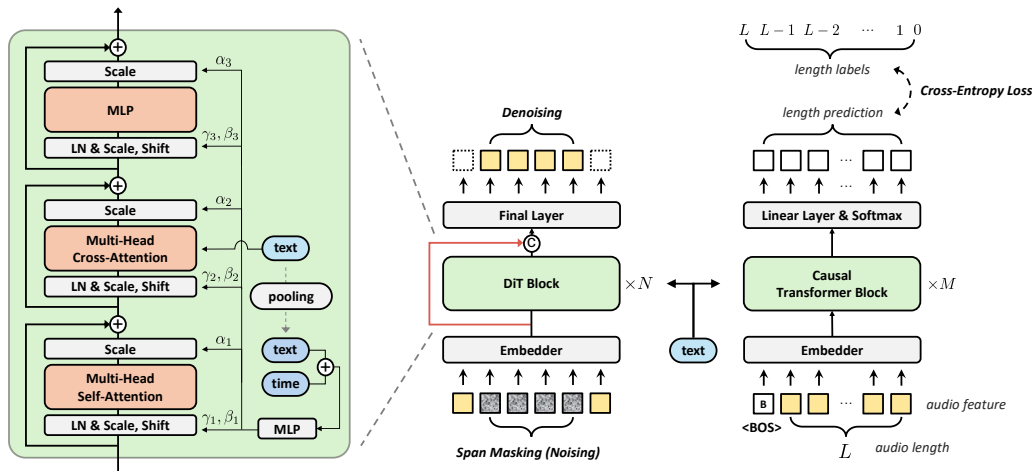


Figure 1: **An overview of DiTTo-TTS.** (*middle*) The LDM backbone is trained to denoise a span-masked noisy segment given its contextual counterpart, without utilizing phoneme and phoneme-level duration (see Section 3.1). (*left*) The inner structure of the DiT block incorporates multi-head cross-attention with global AdaLN (see Section 3.3). (*right*) The speech length predictor is based on causal transformer blocks (see Section 3.2). Both DiT blocks and the speech length predictor employ cross-attention to condition on text representation. Additionally, DiT blocks utilize AdaLN with the mean-pooled text embedding. ‘+’ denotes addition, and ‘c’ represents concatenation. ‘text’ in sky blue oval represents the embedding from text encoder. The red line indicates a long skip connection between the states before and after the DiT blocks. The effectiveness of our design choices is demonstrated in our architecture search (see Section 6.1).

for TTS applications. Consequently, we adopt the Diffusion Transformer (DiT) [10] **to TTS**, naming our method DiTTo-TTS (or simply DiTTo). We also explore the significance of leveraging aligned text and speech representations, showing that performance can be enhanced by either using a text encoder jointly trained with speech data or a speech autoencoder with an auxiliary language modeling objective alongside the reconstruction objective.

Our comprehensive experiments on English-only and multilingual evaluation demonstrate that our model not only simplifies the training process but also achieves superior or comparable zero-shot performance to state-of-the-art models in terms of naturalness, intelligibility, and speaker similarity. The base-sized DiTTo surpasses a state-of-the-art autoregressive model [15], offering an inference speed 4.6 times faster and a model size 3.84 times smaller. Additionally, we demonstrate that our model scales effectively with increases in both data and model sizes.

2 Related Work

Large-scale TTS Recently, large-scale TTS research progresses actively in two main directions: LLM-based autoregressive (AR) TTS and non-autoregressive (Non-AR) TTS. A prominent feature of LLMs is the scalability [16, 17] and their proficiency in zero-shot learning tasks, demonstrating significant capabilities without prior specific training on those tasks [18, 19, 20, 21]. Efforts to replicate LLM’s capability in different modalities have shown progress, including vision [22, 23, 24] and audio [25, 26, 27, 28]. VALL-E [25] employs EnCodec [29] for speech-to-token mapping, posing TTS tasks as AR language modeling tasks, thus enabling zero-shot capabilities in the speech domain. CLaM-TTS [15] introduces Mel-VAE to achieve superior token length compression, and enables a language model to predict multiple tokens simultaneously. Although this approach removes the need for cascaded modeling [25] to manage the number of token streams, their resource-intensive inference processes limit their applications [30]. On the other hand, Non-AR generative models are employed to enhance the efficiency of TTS systems. Voicebox [31] utilizes a flow matching [32] to generate speech, effectively casting the TTS task into a speech infilling task. NaturalSpeech series [12, 33], building upon recent advances in the Latent Diffusion Model (LDM) [7], incorporate auxiliary modules for controllability of various speech attribute such as content, prosody, and timbre. However,

requiring supplementary data beyond speech-transcription pairs hinders scalability. Simple-TTS [13] simplifies the data preparation and training process by removing auxiliary modules and the need for phoneme-level durations. Similarly, E3-TTS [14] follows this approach but does not utilize a pre-trained latent autoencoder. However, both models have limitations in audio quality and impose a fixed length on the target audio, which is a significant constraint for speech generation.

Latent Diffusion Model (LDM) LDM [7] improves modeling efficiency of the diffusion process model [1, 34] by operating in a latent space, achieving remarkable performance in generating realistic samples. Initially applied in image generation, their success is attributed to the reduced dimensionality of the latent space, facilitating efficient training and sampling [7]. Notably, guided diffusion [35, 36] has been expanded to various applications of LDMs, such as image editing [37] and image retrieval [38]. In the field of audio signals, techniques such as style transfer, inpainting, and super-resolution have been explored, along with text-guided audio and speech generation [39, 40]. In the context of TTS, however, applying LDMs to TTS [12, 33] necessitates domain-specific elements such as phonemes, phoneme-level durations, and pitch. This is primarily due to the need for precise temporal alignment between text and speech, as well as the higher fidelity requirements inherent in audio data.

Neural Audio Codec Neural audio codecs, which effectively compress various types of audio using neural networks, are used as part of many TTS systems [12, 15, 25]. Recent advancements employ an encoder-decoder architecture coupled with Residual Vector Quantization (RVQ) [41, 42, 43] to transform raw audio waves into discretized tokens. For example, EnCodec [29] converts 24,000 Hz mono waveforms into 75 Hz latents. With a similar architecture, by focusing the compression specifically on speech rather than general audio signals, Mel-VAE [15] achieves approximately 10.76 Hz latents by compressing the mel-spectrogram. This reduction significantly lowers the computational cost of the speech generation module. Another research direction of improving neural audio codecs for TTS systems is injecting semantic information using large language models (LLMs) [44].

3 Method

We present a latent diffusion model (LDM) for TTS that enables the use of off-the-shelf pre-trained text and speech encoders without relying on speech domain-specific modeling, such as phoneme and duration. Toward this goal, we employ the following two approaches: 1) introducing a **speech length predictor** that predicts the total length of the generated speech without relying on phoneme-level durations or requiring a fixed speech length; and 2) fine-tuning the pre-trained neural audio codec using a pre-trained language model to **enhance the alignment between text and speech** embeddings.

3.1 Preliminary

Diffusion models [1, 34] are a class of generative models that iteratively transform a simple noise distribution into a complex data distribution through a stochastic denoising process. They define a forward process that progressively adds Gaussian noise to the input data as time step increases. The reverse generative process then estimates the added noise to reconstruct the original data. Conditional diffusion models enhance this framework by incorporating additional information, such as text descriptions in text-to-image generation [35, 45] or phonemes and their durations in TTS [11, 46]. While diffusion models can operate directly on real-world data, many of them are applied in the latent space [7, 8, 10, 47]. Thanks to the reduced dimensionality, this approach improves computational efficiency and output quality by allowing diffusion models to focus on the semantic information of the data while the autoencoder handles the high-frequency details that are less perceptible [7].

In our setting, a conditional LDM can be formulated as follows. Given speech audio, an autoencoder produces its latent representation \mathbf{z}_{speech} , and the diffusion model is trained to predict \mathbf{z}_{speech} at each diffusion step $t \in [1, T]$ conditioned on a text token sequence \mathbf{x} . Specifically, the noised latent $\mathbf{z}^{(t)}$ is expressed as $\alpha_t \mathbf{z}_{speech} + \sigma_t \epsilon$, where ϵ is sampled from the standard normal distribution and α_t and σ_t are defined by a noise schedule. Note that $\mathbf{z}^{(1)}$ is \mathbf{z}_{speech} and $\mathbf{z}^{(T)}$ follows the standard normal distribution. We use v -prediction [48] as our model output $\mathbf{v}_\theta(\mathbf{z}^{(t)}, \mathbf{x}, t)$, which predicts $\mathbf{v}^{(t)} := \alpha_t \epsilon - \sigma_t \mathbf{z}^{(t)}$. This setup provides a mean squared error objective as the training loss:

$$\mathcal{L}_{\text{diffusion}} = \mathbb{E}_{t \sim \mathcal{U}(1, T), \epsilon \sim \mathcal{N}(0, I)} \left[\|\mathbf{v}^{(t)} - \mathbf{v}_\theta(\mathbf{z}^{(t)}, \mathbf{x}, t)\|^2 \right].$$

To enrich the contextual information and facilitate zero-shot audio prompting, we incorporate a random span masking into the model training following [31, 49]. We input $\mathbf{z}_{mask}^{(t)} := \mathbf{m} \odot \mathbf{z}^{(t)} +$

$(1 - \mathbf{m}) \odot \mathbf{z}_{speech}$ to the model, where \odot indicates element-wise multiplication and the binary masking \mathbf{m} fully masks with the probability of 0.1 or partially masks a random contiguous segment whose size is between 70% and 100% of data. We also use the binary span masking as an additional input to the model. This allows the model to explicitly identify which part needs to be generated. The inclusion of masking modifies the training loss to:

$$\mathcal{L}_{\text{diffusion}} = \mathbb{E}_{t \sim \mathcal{U}(1, T), \epsilon \sim \mathcal{N}(0, I)} \left[\|\mathbf{m} \odot (\mathbf{v}^{(t)} - \mathbf{v}_{\theta}(\mathbf{z}_{mask}^{(t)}, \mathbf{m}, \mathbf{x}, t))\|^2 \right]. \quad (1)$$

3.2 Model and Training

An overview of our proposed method is presented in Figure 1.

Text Encoder We employ a text encoder from a pre-trained large language model p_{ϕ} , which is parameterized by ϕ . The model was pre-trained to maximize the log-likelihood of the text token sequence $\log p_{\phi}(\mathbf{x})$. The parameters of the model are kept frozen while training the diffusion model for TTS. We denote the output of the text encoder by \mathbf{z}_{text} .

Neural Audio Codec A neural audio codec, which is parameterized by ψ , comprises of three components: 1) an encoder that maps a speech into a sequence of latent representations \mathbf{z}_{speech} ; 2) a vector quantizer converting the latent vector into the discrete code representation; and 3) a decoder that reconstructs the speech from a sequence of the quantized latent representations $\hat{\mathbf{z}}_{speech}$. To enhance alignment between text and speech embeddings, we fine-tune the neural audio codec using the pre-trained language model. We introduce a learnable linear projection $f(\cdot)$ to match the dimension of the latent representation \mathbf{z}_{speech} to the language model’s hidden space. Subsequently, we use this projected embedding in place of the embedding from the pre-trained text encoder within the cross-attention operation of the language model’s decoder. The neural audio codec is fine-tuned with auxiliary loss that infuse semantic content into the generated representations:

$$\mathcal{L}(\psi) = \mathcal{L}_{NAC}(\psi) + \lambda \mathcal{L}_{LM}(\psi), \quad \mathcal{L}_{LM}(\psi) = -\log p_{\phi}(\mathbf{x} | f(\mathbf{z}_{speech})), \quad (2)$$

where $\mathcal{L}_{NAC}(\psi)$ indicate the loss function which is used when the neural audio codec is pre-trained [15]. λ controls the contribution of \mathcal{L}_{LM} , with $\lambda = 0$ indicating the pre-training phase. When $\lambda > 0$, a pre-trained language decoder performs causal language modeling on text token sequences \mathbf{x} , based on the speech latent vector \mathbf{z}_{speech} . While the parameters of language model decoder are fixed, gradients are backpropagated to adjust the linear mappings $f(\mathbf{z}_{speech})$. This training strategy aligns the speech latents with the linguistic latents of the pretrained language model during autoencoding.

Diffusion Model We are given text embedding \mathbf{z}_{text} and speech embedding \mathbf{z}_{speech} . We train the diffusion model $\mathbf{v}_{\theta}(\cdot)$ using the objective in Eq. (1), replacing \mathbf{x} with \mathbf{z}_{text} :

$$\mathcal{L}_{\text{diffusion}} = \mathbb{E}_{t \sim \mathcal{U}(1, T), \epsilon \sim \mathcal{N}(0, I)} \left[\|\mathbf{m} \odot (\mathbf{v}^{(t)} - \mathbf{v}_{\theta}(\mathbf{z}_{mask}^{(t)}, \mathbf{m}, \mathbf{z}_{text}, t))\|^2 \right], \quad (3)$$

where $\mathbf{z}_{mask}^{(t)} = \mathbf{m} \odot \mathbf{z}^{(t)} + (1 - \mathbf{m}) \odot \mathbf{z}_{speech}$ is the masked input latent, \mathbf{m} is the binary span masking, and t is the diffusion time step. We apply classifier-free guidance (CFG) [36] and adopt the diffusion noise schedule from [13].

Speech Length Predictor We introduce a model designed to predict *the total length* of a generated speech for a given text rather than to estimate each phoneme’s duration, and the input noise of diffusion model is set by the length from the speech length predictor at inference time. As shown in Figure 1, we employ an encoder-decoder transformer for the speech length predictor. The encoder processes text input bidirectionally to capture comprehensive textual context, while the decoder, equipped with causal masking to prevent future lookahead, receives an audio token sequence from the encoder of the neural codec for speech prompting at inference time. We use cross-attention mechanisms to integrate text features from the encoder. We use the softmax activation in the final layer to predict the number of tokens to be generated within the given maximum length N . Specifically, the ground truth label for the remaining audio length decreases by one at each subsequent time step. The model is trained separate from the diffusion model, using the cross-entropy loss function.

3.3 Model Architecture

We conduct a comprehensive **model architecture search** to identify the most suitable diffusion-based model for TTS, resulting in the adoption of the Diffusion Transformer (DiT) [10] model (see Section 6.1). We adopt the DiT model in TTS while incorporating recent architectural advancements

for transformer variants, such as the gated linear unit with GELU activation [50], rotary position embeddings [51], and cross-attention with global adaptive layer normalization (AdaLN) [52]. For the latent space, we employ Mel-VAE introduced in [15] which is able to compress audio sequences approximately seven times more than EnCodec [29], yet maintaining superior quality. Due to space limitations, additional details regarding model configurations are provided in Appendix 8.4. We also detail down our noise scheduler and CFG in Appendix 8.6.

4 Experimental Setup

Dataset We employ 82K hours of over 12K unique speakers’ speech-transcript datasets spanning nine languages: English, Korean, German, Dutch, French, Spanish, Italian, Portuguese, and Polish. We train two models: (1) DiTTo-en, a model trained on 55K hour English-only dataset, and (2) DiTTo-multi, a multilingual model trained on 82K hour datasets. Details of each dataset are provided in Appendix 8.1. We follow the data preprocessing methodology described in [15], except that we include all samples without any filtering and exclude speaker metadata from the text prompts. It enables the on-the-fly processing of data with different sampling rates at a uniform rate of 22,050 Hz, approximating audio resampling. We use the same datasets for the speech length predictor with additional LibriSpeech [53] sets: *train-clean-100*, *train-clean-360*, and *train-other-500*. We find that it helps minimize reliance on text normalization (see Appendix 8.1 for discussion). For the evaluation of DiTTo-en and baseline models, we use the *test-clean* subset of LibriSpeech, which consists of speech clips ranging from 4 to 10 seconds with transcripts. For DiTTo-multi, we randomly select 100 examples from the test set of each language dataset, with clip durations ranging from 4 to 20 seconds.

Training Following DiT [10], we train four different sizes of DiTTo: Small (S), Base (B), Large (L), and XLarge (XL). All models are trained on 4 NVIDIA A100 40GB GPUs, and use $T = 1,000$ discrete diffusion steps. The S and B models of DiTTo-en are trained with a maximum token size of 5,120 and a gradient accumulation step of 2 over 1M steps. The L and XL models are trained with a maximum token size of 1,280 and a gradient accumulation step of 4 over 1M steps. The DiTTo-multi model is trained only in the XL configuration, with a maximum token size of 320 and a gradient accumulation step of 4 over 1M steps. The trainable model parameters for DiTTo-en S, B, L, and XL are 41.89M, 151.58M, 507.99M, and 739.97M, respectively, and 790.44M for DiTTo-multi. For the text encoder, we employ SpeechT5 [54]¹ (as in VoiceLDM [40]) and ByT5 [55] in DiTTo-en and DiTTo-multi, respectively. We use the AdamW optimizer [56] with the learning rate of $1e-4$, beta values of (0.9, 0.999), and a weight decay of 0.0. We use a cosine learning rate scheduler with a warmup of 1K steps. Further details of the speech length predictor is provided in Appendix 8.5.

Inference To generate speech, we first input the text and speech prompt into the speech length predictor, which determines the total length of the speech L by adding speech prompt length with the predicted length. Further details about the speech length predictor can be found in Appendix 8.5. The diffusion backbone then generates the latent speech of length L using the same text and speech prompt pair. The generated latent is decoded into mel-spectrograms using the Mel-VAE decoder, and then converted to raw waveform using a pre-trained vocoder, BigVGAN [57].

Metrics We use following objective metrics to evaluate the models: Character Error Rate (CER), Word Error Rate (WER), and Speaker Similarity (SIM) following the procedure outlined in [25] and [15]. CER and WER indicate how intelligible and robust the model is, while SIM represents how well the model captures the speaker’s identity. For subjective metrics, we employ Similarity MOS (SMOS) to measure the speaker similarity between the prompt and the generated speech, and Comparative MOS (CMOS) to assess relative naturalness and audio quality. Details of each metric and evaluation can be found in Appendix 8.2.

Baselines We compare the proposed model with state-of-the-art TTS models including (1) *autoregressive models*: VALL-E [25], SPEAR-TTS [27], CLaM-TTS [15]; (2) *non-autoregressive models*: YourTTS [58], VoiceBox [31]; and (3) *simple diffusion-based models*: Simple-TTS [13]. Since Voicebox [31], VALL-E [25], NaturalSpeech 2 [12], NaturalSpeech 3 [33], Mega-TTS [59], and E3-TTS [14] are not publicly available, we bring the scores reported in the respective paper or samples provided in demo page. Please refer to Appendix 8.3 for details of each model.

Tasks We evaluate our model on two tasks: 1) *continuation*: given a text and an initial 3-second segment of corresponding ground truth speech, the task is to synthesize seamless subsequent speech

¹We use TTS fine-tuned SpeechT5 model from https://huggingface.co/microsoft/speecht5_tts.

Table 1: Performances for the English-only *continuation* task. The boldface indicates the best result, the underline denotes the second best, and the asterisk denotes the score reported in the baseline paper. The inference time indicates the generation time of 10s speech, and #Param. refers to the number of learnable parameters (model size).

Model	Objective Metrics					
	WER ↓	CER ↓	SIM-o ↑	SIM-r ↑	Inference Time ↓	#Param.
Ground Truth	2.2*	0.61*	0.754*	0.754*	n/a	n/a
YourTTS [58]	7.57	3.06	0.3928	-	-	-
VALL-E [25]	3.8*	-	0.452*	0.508*	~6.2s*	302M
Voicebox [31]	2.0*	-	0.593*	0.616*	~6.4s* (64 NFE)	364M
CLaM-TTS [15]	2.36*	0.79*	0.4767*	0.5128*	4.15s*	584M
Simple-TTS [13]	3.86	2.24	0.4413	0.4668	17.897s (250 steps)	243M
DiTTo-en-S	2.01	0.60	0.4544	0.4935	0.884s	42M
DiTTo-en-B	1.87	0.52	0.5535	0.5855	<u>0.903s</u>	152M
DiTTo-en-L	<u>1.85</u>	<u>0.50</u>	0.5596	0.5913	1.479s	508M
DiTTo-en-XL	1.78	0.48	<u>0.5773</u>	<u>0.6075</u>	1.616s	740M

Table 2: Performances for the English-only *cross-sentence* task.

Model	WER ↓	CER ↓	SIM-o ↑	SIM-r ↑
YourTTS [58]	7.92 (7.7*)	3.18	0.3755 (0.337*)	-
VALL-E [25]	5.9*	-	-	0.580*
SPEAR-TTS [27]	-	1.92*	-	0.560*
Voicebox [31]	1.9*	-	0.662*	0.681*
CLaM-TTS [15]	5.11*	2.87*	0.4951*	0.5382*
Simple-TTS [13]	4.09 (3.4*)	2.11	0.5026	0.5305 (0.514*)
DiTTo-en-S	3.07	1.08	0.4984	0.5373
DiTTo-en-B	2.74	0.98	0.5977	0.6281
DiTTo-en-L	2.69	<u>0.91</u>	0.6050	0.6355
DiTTo-en-XL	<u>2.56</u>	0.89	<u>0.6270</u>	<u>0.6554</u>

that reads the text in the style of the provided speech segment; 2) *cross-sentence*: given a text, a 3-second speech segment, and its corresponding transcript (which differs from the given text), the task is to synthesize speech that reads the text in the style of the provided 3-second speech.

5 Experimental Results

5.1 Comparison with Baselines

For *English-only Evaluation*, we evaluate the performances of DiTTo-en across *continuation* and *cross-sentence* tasks. Recall that DiTTo-en is the model trained on 55K English-only dataset. Following the evaluation setting in [25], we employ a subset of the LibriSpeech test-clean dataset. This subset comprises speech clips ranging from 4 to 10 seconds, each with a corresponding transcript. We use open-sourced checkpoints of YourTTS² and Simple-TTS³ for evaluations, and the official checkpoint of CLaM-TTS. When conducting subjective evaluations, all samples are resampled to 16,000 Hz. Further details can be found in Appendix 8.3.

Table 1 and 2 present the results of the *continuation* and *cross-sentence* tasks, respectively. Our model demonstrates excellent performance across all measures, consistently ranking either first or second. Specifically, the DiTTo-en base (B) model outperforms CLaM-TTS, a state-of-the-art (SOTA) autoregressive (AR) model, in terms of naturalness, intelligibility, and speaker similarity, while achieving an inference speed that is 4.6 times faster with 3.84 times smaller model size. Despite

²<https://github.com/Edresson/YourTTS>

³<https://github.com/asappresearch/simple-tts>

Table 3: Human evaluations on *cross-sentence* task with 40 LibriSpeech test-clean speakers show DiTTo-en-XL surpasses the baseline in quality, intelligibility, similarity, and naturalness, nearing Ground Truth. SMOS scores include a 95% confidence interval. The boldface indicates the best result and *recon* indicates the reconstructed audio by Mel-VAE followed by vocoder.

Model	SMOS	CMOS
Simple-TTS [13]	2.15±0.19	-1.64
CLaM-en [15]	3.42±0.16	-0.52
DiTTo-en-XL	3.91±0.16	0.00
Ground Truth (<i>recon</i>)	4.07±0.14	+0.11
Ground Truth	4.08±0.14	+0.13

Table 4: Performances of English-only *cross-sentence* task for Mel-VAE++. All models are trained on MLS English and consumed ground truth length during sampling. The boldface indicates the best result within the same text encoder setting, and † represents the best result across all cases.

Text Encoder	Neural Audio Codec	WER ↓	CER ↓	SIM-o ↑	SIM-r ↑
SpeechT5	Mel-VAE	3.07	1.15	0.5423	0.5858
SpeechT5	Mel-VAE++	2.99†	1.06†	0.5364	0.5982†
ByT5-base	Mel-VAE	6.22	3.82	0.5482†	0.5945
ByT5-base	Mel-VAE++	3.11	1.17	0.5323	0.5965

its simplicity, our model achieves performance comparable to more complex a non-autoregressive (Non-AR) SOTA TTS model which use a phoneme-level duration modeling. Additionally, DiTTo-en surpasses a simple diffusion-based model, Simple-TTS, further demonstrating its effectiveness.

Table 3 presents the results of subjective evaluations. DiTTo-en significantly outperforms the baseline models, Simple-TTS and CLaM-en, and achieves performance comparable to the ground truth in terms of speaker similarity (as measured by SMOS) as well as naturalness, quality, and intelligibility (as assessed by CMOS). In Appendix 8.8, Table 9 shows the results of the subjective evaluation compared to the baseline demo samples. We use the provided voice samples as is (as detailed down in Appendix 8.3), and our model operates at 22,050 Hz. Our model surpasses all models except NaturalSpeech 3 in SMOS and all models except Voicebox in CMOS.

For *Multilingual Evaluations*, we provide the result in Appendix 8.9 due to space constraints. Table 10 presents the result of the *continuation* task for DiTTo-multi. DiTTo-multi shows better or comparable performances compared to CLaM-TTS performances, as reported in Table 11.

5.2 Scaling Model Size

We train 4 models of different size on 55K hour English-only datasets, which are referred to as small (S), base (B), Large (L), and XLarge (XL). Detailed model configurations are provided in Appendix 8.4. As shown in Table 3, we observe the performance improvement as the model size increases.

5.3 Aligned Text-Speech Embeddings Improve Performances

DiTTo uses cross-attention for text conditioning, which can be influenced by the distance between text and speech representations. To validate the effect of aligned text-speech embeddings, we train DiTTo variants for 200K steps on the MLS English subset (referred to as DiTTo-mls) with two different text encoders: 1) SpeechT5 [54], which is trained jointly on English-only text and corresponding speech, and 2) ByT5 [55] (we use ByT5-base), which is trained solely on a large corpus of multilingual text. In Table 4, we observe that DiTTo-mls trained with SpeechT5 outperforms the model trained with ByT5-base. Given that the encoder size for SpeechT5 is 85M and for ByT5-base is 415M, and that ByT5 trains on a significantly larger dataset, this indicates that aligning text embeddings with speech embeddings effectively enhances TTS performance, independent of the model or data size.

Building on this insight, we fine-tune Mel-VAE on the same MLS dataset for 200K steps by setting $\lambda > 0$ in Eq. (2). This process results in two fine-tuned models, referred to as Mel-VAE++, each aligned with SpeechT5 and ByT5, respectively. Further experiments, presented in Appendix 8.7, demonstrate that DiTTo-mls using Mel-VAE++ outperforms the version using Mel-VAE. This effect

Table 5: Performances of English-only cross-sentence task for ablation study. All models use SpeechT5 as text encoder and original Mel-VAE as audio latent codec, and consume ground truth length during sampling. We set the diffusion steps to 250 for WER and SIM-r and 25 for Inference Time, noise schedule scale shift to 0.3, and classifier-free guidance scale to 5.0. Results confirm the effectiveness of the architectural design of our model. The boldface indicates the best result.

Model	WER ↓	SIM-r ↑	Inference Time ↓
<i>U-Net</i>	3.70	0.3890	1.328s
<i>Flat-U-Net</i>	2.97	0.5471	1.310s
DiTTo- <i>local-adaln</i>	3.38	0.5673	0.937s
DiTTo- <i>uvit-skip</i>	3.17	0.5848	0.940s
DiTTo- <i>no-skip</i>	3.30	0.5727	0.905s
Simple-TTS (from Table 2)	4.09	0.5305	1.982s
DiTTo	2.93	0.5877	0.903s
DiTTo- <i>encodec</i>	4.19	0.5460	n/a
DiTTo- <i>fixed-length (trimmed)</i>	3.72	0.5707	1.303s

is more pronounced with the DiTTo-mls and Mel-VAE++ pair aligned with ByT5 than with SpeechT5, because SpeechT5’s text embeddings are already aligned with speech embeddings during pre-training. Aggregating all results, we can conclude that fine-tuning the neural audio codec, rather than the language model, is sufficient to enhance alignment and subsequently improve TTS performance. This approach offers a significant advantage since fine-tuning the language model is more time-consuming.

6 Ablation Study

We conduct an ablation study to analyze the proposed method. First, we evaluate the performance changes associated with various options for the model structure, confirming the validity of our choices. Next, we perform a search for hyperparameters, including the number of diffusion steps. All models train for 200K steps using the MLS English subset in the base (B) configuration. We adopt the same span masking strategy, utilize L1 loss, and constrain the training data to 20 seconds as described in [13]. Other hyperparameters remain consistent with those used in DiTTo training.

6.1 Model Architecture Search

As listed in Table 5, we consider several model architecture options, and our final design demonstrates optimal performance in WER and SIM-r while showing the fastest inference time. We begin with the U-Net diffusion model (referred to as *U-Net*). We train the U-Audio Transformer (U-AT) proposed by [13] on the Mel-VAE latent, where the input latent undergoes an 8-fold down/up sampling. Given that Mel-VAE already compresses about seven times more than EnCodec, this additional compression results in significant information loss and poor output quality. Next, we eliminate the down/up sampling (referred to as *Flat-U-Net*), which proves to be more suitable choice than U-Net but still leaves room for improvement. Subsequently, we remove the residual and convolution block, making our model resemble the DiT architecture. We then modify AdaLN to be shared (referred to as DiTTo-*local-adaln*), as implemented in Pixart-alpha [9]. This reduces model parameters by 30.5% (for XL models) and surprisingly improves performance as well.

Additionally, we add a long skip connection to DiT inspired by U-Net. Notably, connecting the hidden layers inside the transformer block as in U-ViT [60] (referred to as DiTTo-*uvit-skip*) or without any skip connection (referred to as DiTTo-*no-skip*) is less effective in terms of model convergence than a residual connection that links before and after the transformer block (referred to as DiTTo). Training on the latent from EnCodec instead of Mel-VAE (referred to as DiTTo-*encodec*) results in performance degradation, confirming that Mel-VAE and DiT structures complement each other.

Finally, we confirm that fixing the input/output sequence length (referred to as DiTTo-*fixed-length (trimmed)*), where we have to manually trim the output speech to remove silence at the end, degrades performance compared to variable-length modeling. Furthermore, the variable-length modeling enables speech rate control by changing the total length of the generated speech latent, as illustrated in Figure 2. Our model design shows the best performance not only in both WER and SIM-r, but also

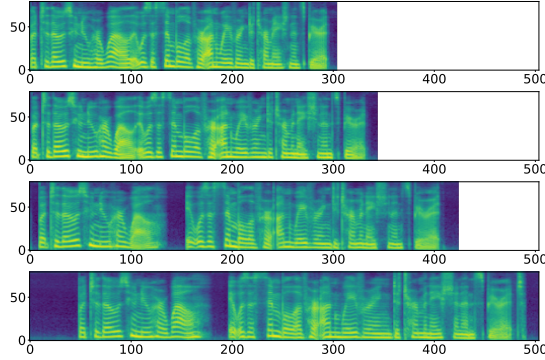


Figure 2: **Speech rate controllability** is illustrated through mel-spectrograms of generated speech at various rates. The speech rate decreases from top to bottom, achieved by adjusting the latent length from 38 to 63. The transcript is "But to those who knew her well, it was a symbol of her unwavering determination and spirit." The x -axis represents the length, and the y -axis represents the channels of the mel-spectrogram. Speech samples are available at <https://ditto-tts.github.io>.

inference time. Note that we can not measure the total inference time of DiTTo-*encodec* since there is no speech length predictor that bases its predictions on EnCodec audio embeddings.

6.2 Noise Schedule Scale and Sampling

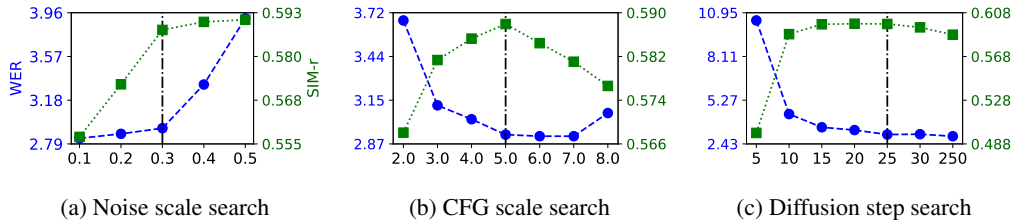


Figure 3: A configuration search results for (a) scale-shift of the noise scheduler, (b) classifier-free guidance (CFG) scale, and (c) diffusion step search. We can conclude to set scale-shift to 0.3 from (a) and CFG scale to 5.0 from (b), and diffusion steps to 25 from (c).

We conduct a hyperparameter search for three components regarding noise schedule and sampling: (a) the scale-shift of the noise scheduler by training five different models with scales ranging from 0.1 to 0.5 (Figure 3a) as visualized in Figure 5 in Appendix 8.6, (b) the classifier-free guidance (CFG) scale during inference (Figure 3b), and (c) the number of diffusion steps during inference (Figure 3c). In these figures, The blue *dashed* line with circle marker represents the **WER**, and the green *dotted* line with square marker represents the **SIM-r**. The selected values in each experiment are marked with vertical black dash-dot lines. From the hyperparameter search, we set the noise scale and the CFG scale to 0.3 and 5.0, respectively. Notably, 25 diffusion steps are sufficient to produce high-fidelity outputs, and we observe that performance gaps among different steps diminish with further training.

7 Conclusion

We presented DiTTo-TTS, a latent diffusion model for text-to-speech (TTS) that leverages cross-attention and the prediction of the total length of latent speech representations to achieve text-speech alignment. We demonstrated that the proposed method shows exceptional zero-shot performance in naturalness, intelligibility, and speaker similarity, all without relying on domain-specific elements such as phonemes and durations, while simplifying the training process as well. In the process of obtaining this result, we also found that fine-tuning a speech autoencoder with an auxiliary language modeling objective can significantly enhance the text-speech alignment. Moreover, DiTTo-TTS shows effective scalability with respect to data and model sizes. Our future work includes: 1) exploring various noise schedules to improve output quality and distillation methods to reduce inference times; 2) enhancing pronunciation accuracy by improving character input normalization; and 3) enabling DiTTo to understand and learn from natural language instructions.

Acknowledgment

The authors would like to express our gratitude to Kangwook Lee for the valuable discussions. We also extend our thanks to Seungjun Chung for his thorough proofreading of the paper, and to Beomsoo Kim and Gibum Seo for their essential support in data handling and verification.

References

- [1] Jonathan Ho, Ajay Jain, and Pieter Abbeel. Denoising diffusion probabilistic models. In *Advances in Neural Information Processing Systems (NeurIPS)*, pages 6840–6851, 2020.
- [2] Yang Song, Jascha Sohl-Dickstein, Diederik P Kingma, Abhishek Kumar, Stefano Ermon, and Ben Poole. Score-based generative modeling through stochastic differential equations. In *International Conference on Learning Representations (ICLR)*, 2020.
- [3] Uriel Singer, Adam Polyak, Thomas Hayes, Xi Yin, Jie An, Songyang Zhang, Qiyuan Hu, Harry Yang, Oron Ashual, Oran Gafni, et al. Make-a-video: Text-to-video generation without text-video data. In *International Conference on Learning Representations (ICLR)*, 2022.
- [4] Omer Bar-Tal, Hila Chefer, Omer Tov, Charles Herrmann, Roni Paiss, Shiran Zada, Ariel Ephrat, Junhwa Hur, Yuanzhen Li, Tomer Michaeli, et al. Lumiere: A space-time diffusion model for video generation. *arXiv preprint arXiv:2401.12945*, 2024.
- [5] Nanxin Chen, Yu Zhang, Heiga Zen, Ron J Weiss, Mohammad Norouzi, and William Chan. Wavegrad: Estimating gradients for waveform generation. In *International Conference on Learning Representations (ICLR)*, 2020.
- [6] Zhifeng Kong, Wei Ping, Jiaji Huang, Kexin Zhao, and Bryan Catanzaro. Diffwave: A versatile diffusion model for audio synthesis. In *International Conference on Learning Representations (ICLR)*, 2020.
- [7] Robin Rombach, Andreas Blattmann, Dominik Lorenz, Patrick Esser, and Björn Ommer. High-resolution image synthesis with latent diffusion models. In *Proceedings of the IEEE/CVF Conference on Computer Vision and Pattern Recognition*, pages 10684–10695, 2022.
- [8] Andreas Blattmann, Robin Rombach, Huan Ling, Tim Dockhorn, Seung Wook Kim, Sanja Fidler, and Karsten Kreis. Align your latents: High-resolution video synthesis with latent diffusion models. In *Proceedings of the IEEE/CVF Conference on Computer Vision and Pattern Recognition*, pages 22563–22575, 2023.
- [9] Junsong Chen, YU Jincheng, GE Chongjian, Lewei Yao, Enze Xie, Zhongdao Wang, James Kwok, Ping Luo, Huchuan Lu, and Zhenguo Li. Pixart-*alpha*: Fast training of diffusion transformer for photorealistic text-to-image synthesis. In *International Conference on Learning Representations (ICLR)*, 2023.
- [10] William Peebles and Saining Xie. Scalable diffusion models with transformers. In *Proceedings of the IEEE/CVF International Conference on Computer Vision*, pages 4195–4205, 2023.
- [11] Vadim Popov, Ivan Vovk, Vladimir Gogoryan, Tasnima Sadekova, and Mikhail Kudinov. GradTts: A diffusion probabilistic model for text-to-speech. In *International Conference on Machine Learning (ICML)*, pages 8599–8608. PMLR, 2021.
- [12] Kai Shen, Zeqian Ju, Xu Tan, Eric Liu, Yichong Leng, Lei He, Tao Qin, Jiang Bian, et al. NaturalSpeech 2: Latent diffusion models are natural and zero-shot speech and singing synthesizers. In *International Conference on Learning Representations (ICLR)*, 2023.
- [13] Justin Lovelace, Soham Ray, Kwangyoun Kim, Kilian Q Weinberger, and Felix Wu. Simple-TTS: End-to-end text-to-speech synthesis with latent diffusion, 2024.
- [14] Yuan Gao, Nobuyuki Morioka, Yu Zhang, and Nanxin Chen. E3 tts: Easy end-to-end diffusion-based text to speech. In *2023 IEEE Automatic Speech Recognition and Understanding Workshop (ASRU)*, pages 1–8. IEEE, 2023.
- [15] Jaehyeon Kim, Keon Lee, Seungjun Chung, and Jaewoong Cho. CLam-TTS: Improving neural codec language model for zero-shot text-to-speech. In *International Conference on Learning Representations (ICLR)*, 2024.

- [16] Mohammad Shoeybi, Mostofa Patwary, Raul Puri, Patrick LeGresley, Jared Casper, and Bryan Catanzaro. Megatron-lm: Training multi-billion parameter language models using model parallelism. *CoRR*, abs/1909.08053, 2019.
- [17] Jared Kaplan, Sam McCandlish, Tom Henighan, Tom B. Brown, Benjamin Chess, Rewon Child, Scott Gray, Alec Radford, Jeffrey Wu, and Dario Amodei. Scaling laws for neural language models. *CoRR*, abs/2001.08361, 2020.
- [18] Tom Brown, Benjamin Mann, Nick Ryder, Melanie Subbiah, Jared D Kaplan, Prfulla Dhariwal, Arvind Neelakantan, Pranav Shyam, Girish Sastry, Amanda Askell, Sandhini Agarwal, Ariel Herbert-Voss, Gretchen Krueger, Tom Henighan, Rewon Child, Aditya Ramesh, Daniel Ziegler, Jeffrey Wu, Clemens Winter, Chris Hesse, Mark Chen, Eric Sigler, Mateusz Litwin, Scott Gray, Benjamin Chess, Jack Clark, Christopher Berner, Sam McCandlish, Alec Radford, Ilya Sutskever, and Dario Amodei. Language models are few-shot learners. In H. Larochelle, M. Ranzato, R. Hadsell, M.F. Balcan, and H. Lin, editors, *Advances in Neural Information Processing Systems (NeurIPS)*, volume 33, pages 1877–1901. Curran Associates, Inc., 2020.
- [19] Hugo Touvron, Thibaut Lavril, Gautier Izacard, Xavier Martinet, Marie-Anne Lachaux, Timothée Lacroix, Baptiste Rozière, Naman Goyal, Eric Hambro, Faisal Azhar, et al. Llama: Open and efficient foundation language models. *arXiv preprint arXiv:2302.13971*, 2023.
- [20] OpenAI. ChatGPT. <https://openai.com/blog/chatgpt/>, 2022.
- [21] OpenAI. Gpt-4 technical report, 2023.
- [22] Haotian Liu, Chunyuan Li, Qingyang Wu, and Yong Jae Lee. Visual instruction tuning. *Advances in Neural Information Processing Systems (NeurIPS)*, 36, 2024.
- [23] Junnan Li, Dongxu Li, Silvio Savarese, and Steven Hoi. BLIP-2: Bootstrapping language-image pre-training with frozen image encoders and large language models. In Andreas Krause, Emma Brunskill, Kyunghyun Cho, Barbara Engelhardt, Sivan Sabato, and Jonathan Scarlett, editors, *International Conference on Machine Learning (ICML)*, volume 202 of *Proceedings of Machine Learning Research*, pages 19730–19742. PMLR, 23–29 Jul 2023.
- [24] Yassir Fathullah, Chunyang Wu, Egor Lakomkin, Junteng Jia, Yuan Shangguan, Ke Li, Jinxi Guo, Wenhan Xiong, Jay Mahadeokar, Ozlem Kalinli, et al. Prompting large language models with speech recognition abilities. In *ICASSP 2024-2024 IEEE International Conference on Acoustics, Speech and Signal Processing (ICASSP)*, pages 13351–13355. IEEE, 2024.
- [25] Chengyi Wang, Sanyuan Chen, Yu Wu, Ziqiang Zhang, Long Zhou, Shujie Liu, Zhuo Chen, Yanqing Liu, Huaming Wang, Jinyu Li, et al. Neural codec language models are zero-shot text to speech synthesizers. *arXiv preprint arXiv:2301.02111*, 2023.
- [26] Zalán Borsos, Raphaël Marinier, Damien Vincent, Eugene Kharitonov, Olivier Pietquin, Matt Sharifi, Dominik Roblek, Olivier Teboul, David Grangier, Marco Tagliasacchi, and Neil Zeghidour. Audioldm: A language modeling approach to audio generation. *IEEE/ACM Transactions on Audio, Speech, and Language Processing*, 31:2523–2533, 2023.
- [27] Eugene Kharitonov, Damien Vincent, Zalán Borsos, Raphaël Marinier, Sertan Girgin, Olivier Pietquin, Matt Sharifi, Marco Tagliasacchi, and Neil Zeghidour. Speak, Read and Prompt: High-Fidelity Text-to-Speech with Minimal Supervision. *Transactions of the Association for Computational Linguistics*, 11:1703–1718, 12 2023.
- [28] Yunfei Chu, Jin Xu, Xiaohuan Zhou, Qian Yang, Shiliang Zhang, Zhijie Yan, Chang Zhou, and Jingren Zhou. Qwen-audio: Advancing universal audio understanding via unified large-scale audio-language models. *arXiv preprint arXiv:2311.07919*, 2023.
- [29] Alexandre Défossez, Jade Copet, Gabriel Synnaeve, and Yossi Adi. High fidelity neural audio compression. *Transactions on Machine Learning Research*, 2023.
- [30] Joshua Ainslie, James Lee-Thorp, Michiel de Jong, Yury Zemlyanskiy, Federico Lebron, and Sumit Sanghai. GQA: Training generalized multi-query transformer models from multi-head checkpoints. In Houda Bouamor, Juan Pino, and Kalika Bali, editors, *Proceedings of the 2023 Conference on Empirical Methods in Natural Language Processing*, pages 4895–4901, Singapore, December 2023. Association for Computational Linguistics.
- [31] Matthew Le, Apoorv Vyas, Bowen Shi, Brian Karrer, Leda Sari, Rashel Moritz, Mary Williamson, Vimal Manohar, Yossi Adi, Jay Mahadeokar, and Wei-Ning Hsu. Voicebox:

- Text-guided multilingual universal speech generation at scale. In A. Oh, T. Neumann, A. Globerson, K. Saenko, M. Hardt, and S. Levine, editors, *Advances in Neural Information Processing Systems (NeurIPS)*, volume 36, pages 14005–14034. Curran Associates, Inc., 2023.
- [32] Yaron Lipman, Ricky TQ Chen, Heli Ben-Hamu, Maximilian Nickel, and Matthew Le. Flow matching for generative modeling. In *International Conference on Learning Representations (ICLR)*, 2022.
- [33] Zeqian Ju, Yuancheng Wang, Kai Shen, Xu Tan, Detai Xin, Dongchao Yang, Yanqing Liu, Yichong Leng, Kaitao Song, Siliang Tang, Zhizheng Wu, Tao Qin, Xiang-Yang Li, Wei Ye, Shikun Zhang, Jiang Bian, Lei He, Jinyu Li, and Sheng Zhao. Naturalspeech 3: Zero-shot speech synthesis with factorized codec and diffusion models. In *International Conference on Machine Learning (ICML)*, June 2024.
- [34] Jiaming Song, Chenlin Meng, and Stefano Ermon. Denoising diffusion implicit models. In *International Conference on Learning Representations (ICLR)*, 2021.
- [35] Prafulla Dhariwal and Alexander Nichol. Diffusion models beat gans on image synthesis. *Advances in Neural Information Processing Systems (NeurIPS)*, 34:8780–8794, 2021.
- [36] Jonathan Ho and Tim Salimans. Classifier-free diffusion guidance. In *NeurIPS 2021 Workshop on Deep Generative Models and Downstream Applications*, 2021.
- [37] Tim Brooks, Aleksander Holynski, and Alexei A Efros. Instructpix2pix: Learning to follow image editing instructions. In *Proceedings of the IEEE/CVF Conference on Computer Vision and Pattern Recognition*, pages 18392–18402. IEEE, 2023.
- [38] Geonmo Gu, Sanghyuk Chun, Wonjae Kim, HeeJae Jun, Yoohoon Kang, and Sangdoon Yun. Compodiff: Versatile composed image retrieval with latent diffusion. *arXiv preprint arXiv:2303.11916*, 2023.
- [39] Haohe Liu, Zehua Chen, Yi Yuan, Xinhao Mei, Xubo Liu, Danilo Mandic, Wenwu Wang, and Mark D Plumbley. Audioldm: Text-to-audio generation with latent diffusion models. In *International Conference on Machine Learning (ICML)*, pages 21450–21474. PMLR, 2023.
- [40] Yeonghyeon Lee, Inmo Yeon, Juhan Nam, and Joon Son Chung. Voiceldm: Text-to-speech with environmental context. In *ICASSP 2024-2024 IEEE International Conference on Acoustics, Speech and Signal Processing (ICASSP)*, pages 12566–12571. IEEE, 2024.
- [41] Robert Gray. Vector quantization. *IEEE Assp Magazine*, 1(2):4–29, 1984.
- [42] A Vasuki and PT Vanathi. A review of vector quantization techniques. *IEEE Potentials*, 25(4):39–47, 2006.
- [43] Doyup Lee, Chiheon Kim, Saehoon Kim, Minsu Cho, and Wook-Shin Han. Autoregressive image generation using residual quantization. In *Proceedings of the IEEE/CVF Conference on Computer Vision and Pattern Recognition*, pages 11523–11532, 2022.
- [44] Xin Zhang, Dong Zhang, Shimin Li, Yaqian Zhou, and Xipeng Qiu. Speeche tokenizer: Unified speech tokenizer for speech language models. In *International Conference on Learning Representations (ICLR)*, 2024.
- [45] Chitwan Saharia, William Chan, Saurabh Saxena, Lala Li, Jay Whang, Emily L Denton, Kamyar Ghasemipour, Raphael Gontijo Lopes, Burcu Karagol Ayan, Tim Salimans, et al. Photorealistic text-to-image diffusion models with deep language understanding. *Advances in Neural Information Processing Systems (NeurIPS)*, 35:36479–36494, 2022.
- [46] Heeseung Kim, Sungwon Kim, and Sungroh Yoon. Guided-tts: A diffusion model for text-to-speech via classifier guidance. In *International Conference on Machine Learning (ICML)*, pages 11119–11133. PMLR, 2022.
- [47] Deepanway Ghosal, Navonil Majumder, Ambuj Mehrish, and Soujanya Poria. Text-to-audio generation using instruction guided latent diffusion model. In *Proceedings of the 31st ACM International Conference on Multimedia*, MM '23, page 3590–3598, New York, NY, USA, 2023. Association for Computing Machinery.
- [48] Tim Salimans and Jonathan Ho. Progressive distillation for fast sampling of diffusion models. In *International Conference on Learning Representations (ICLR)*, 2022.
- [49] Apoorv Vyas, Bowen Shi, Matthew Le, Andros Tjandra, Yi-Chiao Wu, Baishan Guo, Jiemin Zhang, Xinyue Zhang, Robert Adkins, William Ngan, et al. Audiobox: Unified audio generation with natural language prompts. *arXiv preprint arXiv:2312.15821*, 2023.

- [50] Noam Shazeer. Glu variants improve transformer. *arXiv preprint arXiv:2002.05202*, 2020.
- [51] Jianlin Su, Murtadha Ahmed, Yu Lu, Shengfeng Pan, Wen Bo, and Yunfeng Liu. Roformer: Enhanced transformer with rotary position embedding. *Neurocomputing*, 568:127063, 2024.
- [52] Shoufa Chen, Mengmeng Xu, Jiawei Ren, Yuren Cong, Sen He, Yanping Xie, Animesh Sinha, Ping Luo, Tao Xiang, and Juan-Manuel Perez-Rua. Gentron: Diffusion transformers for image and video generation. In *Proceedings of the IEEE/CVF Conference on Computer Vision and Pattern Recognition*, pages 6441–6451, June 2024.
- [53] Vassil Panayotov, Guoguo Chen, Daniel Povey, and Sanjeev Khudanpur. Librispeech: an asr corpus based on public domain audio books. In *ICASSP 2015-2015 IEEE International Conference on Acoustics, Speech and Signal Processing (ICASSP)*, pages 5206–5210. IEEE, 2015.
- [54] Junyi Ao, Rui Wang, Long Zhou, Chengyi Wang, Shuo Ren, Yu Wu, Shujie Liu, Tom Ko, Qing Li, Yu Zhang, et al. Specht5: Unified-modal encoder-decoder pre-training for spoken language processing. In *Proceedings of the 60th Annual Meeting of the Association for Computational Linguistics (Volume 1: Long Papers)*, pages 5723–5738, 2022.
- [55] Linting Xue, Aditya Barua, Noah Constant, Rami Al-Rfou, Sharan Narang, Mihir Kale, Adam Roberts, and Colin Raffel. ByT5: Towards a token-free future with pre-trained byte-to-byte models. *Transactions of the Association for Computational Linguistics*, 10:291–306, 2022.
- [56] Ilya Loshchilov and Frank Hutter. Decoupled weight decay regularization. In *International Conference on Learning Representations (ICLR)*, 2019.
- [57] Sang gil Lee, Wei Ping, Boris Ginsburg, Bryan Catanzaro, and Sungroh Yoon. BigVGAN: A universal neural vocoder with large-scale training. In *International Conference on Learning Representations (ICLR)*, 2023.
- [58] Edresson Casanova, Julian Weber, Christopher D Shulby, Arnaldo Candido Junior, Eren Gölge, and Moacir A Ponti. Yourtts: Towards zero-shot multi-speaker tts and zero-shot voice conversion for everyone. In *International Conference on Machine Learning (ICML)*, pages 2709–2720. PMLR, 2022.
- [59] Ziyue Jiang, Yi Ren, Zhenhui Ye, Jinglin Liu, Chen Zhang, Qian Yang, Shengpeng Ji, Rongjie Huang, Chunfeng Wang, Xiang Yin, et al. Mega-tts: Zero-shot text-to-speech at scale with intrinsic inductive bias. *arXiv preprint arXiv:2306.03509*, 2023.
- [60] Fan Bao, Shen Nie, Kaiwen Xue, Yue Cao, Chongxuan Li, Hang Su, and Jun Zhu. All are worth words: A vit backbone for diffusion models. In *Proceedings of the IEEE/CVF Conference on Computer Vision and Pattern Recognition*, pages 22669–22679. IEEE Computer Society, 2023.
- [61] Vineel Pratap, Qiantong Xu, Anuroop Sriram, Gabriel Synnaeve, and Ronan Collobert. MLS: A Large-Scale Multilingual Dataset for Speech Research. In *Interspeech*, pages 2757–2761, 2020.
- [62] Guoguo Chen, Shuzhou Chai, Guan-Bo Wang, Jiayu Du, Wei-Qiang Zhang, Chao Weng, Dan Su, Daniel Povey, Jan Trmal, Junbo Zhang, Mingjie Jin, Sanjeev Khudanpur, Shinji Watanabe, Shuaijiang Zhao, Wei Zou, Xiangang Li, Xuchen Yao, Yongqing Wang, Zhao You, and Zhiyong Yan. GigaSpeech: An Evolving, Multi-Domain ASR Corpus with 10,000 Hours of Transcribed Audio. In *Interspeech*, pages 3670–3674, 2021.
- [63] Yuma Koizumi, Heiga Zen, Shigeki Karita, Yifan Ding, Kohei Yatabe, Nobuyuki Morioka, Michiel Bacchiani, Yu Zhang, Wei Han, and Ankur Bapna. LibriTTS-R: A Restored Multi-Speaker Text-to-Speech Corpus. In *Interspeech*, pages 5496–5500, 2023.
- [64] Heiga Zen, Viet Dang, Rob Clark, Yu Zhang, Ron J. Weiss, Ye Jia, Zhifeng Chen, and Yonghui Wu. LibriTTS: A Corpus Derived from LibriSpeech for Text-to-Speech. In *Interspeech*, pages 1526–1530, 2019.
- [65] Christophe Veaux, Junichi Yamagishi, Kirsten MacDonald, et al. Superseded-cstr vctk corpus: English multi-speaker corpus for cstr voice cloning toolkit. *University of Edinburgh. The Centre for Speech Technology Research (CSTR)*, 2016.
- [66] Keith Ito and Linda Johnson. The lj speech dataset. <https://keithito.com/LJ-Speech-Dataset/>, 2017.
- [67] Tu Anh Nguyen, Wei-Ning Hsu, Antony D’Avirro, Bowen Shi, Itai Gat, Maryam Fazal-Zarani, Tal Remez, Jade Copet, Gabriel Synnaeve, Michael Hassid, Felix Kreuk, Yossi Adi, and

- Emmanuel Dupoux. Espresso: A Benchmark and Analysis of Discrete Expressive Speech Resynthesis. In *Interspeech*, pages 4823–4827, 2023.
- [68] Jeong-Uk Bang, Seung Yun, Seung-Hi Kim, Mu-Yeol Choi, Min-Kyu Lee, Yeo-Jeong Kim, Dong-Hyun Kim, Jun Park, Young-Jik Lee, and Sang-Hun Kim. Kspnspeech: Korean spontaneous speech corpus for automatic speech recognition. *Applied Sciences*, 10(19):6936, 2020.
- [69] Wei-Ning Hsu, Benjamin Bolte, Yao-Hung Hubert Tsai, Kushal Lakhota, Ruslan Salakhutdinov, and Abdelrahman Mohamed. Hubert: Self-supervised speech representation learning by masked prediction of hidden units. *IEEE/ACM Transactions on Audio, Speech, and Language Processing*, 29:3451–3460, 2021.
- [70] Alec Radford, Jong Wook Kim, Tao Xu, Greg Brockman, Christine McLeavey, and Ilya Sutskever. Robust speech recognition via large-scale weak supervision. In *International Conference on Machine Learning (ICML)*, pages 28492–28518. PMLR, 2023.
- [71] Yang Zhang, Evelina Bakhturina, and Boris Ginsburg. NeMo (Inverse) Text Normalization: From Development to Production. In *Interspeech*, pages 4857–4859, 2021.
- [72] Evelina Bakhturina, Yang Zhang, and Boris Ginsburg. Shallow Fusion of Weighted Finite-State Transducer and Language Model for Text Normalization. In *Interspeech*, 2022.
- [73] Sanyuan Chen, Chengyi Wang, Zhengyang Chen, Yu Wu, Shujie Liu, Zhuo Chen, Jinyu Li, Naoyuki Kanda, Takuya Yoshioka, Xiong Xiao, et al. Wavlm: Large-scale self-supervised pre-training for full stack speech processing. *IEEE Journal of Selected Topics in Signal Processing*, 16(6):1505–1518, 2022.
- [74] Jaehyeon Kim, Jungil Kong, and Juhee Son. Conditional variational autoencoder with adversarial learning for end-to-end text-to-speech. In *International Conference on Machine Learning (ICML)*, pages 5530–5540. PMLR, 2021.
- [75] Gemma Team, Thomas Mesnard, Cassidy Hardin, Robert Dadashi, Surya Bhupatiraju, Shreya Pathak, Laurent Sifre, Morgane Rivière, Mihir Sanjay Kale, Juliette Love, et al. Gemma: Open models based on gemini research and technology. *arXiv preprint arXiv:2403.08295*, 2024.
- [76] Olaf Ronneberger, Philipp Fischer, and Thomas Brox. U-net: Convolutional networks for biomedical image segmentation. In Nassir Navab, Joachim Hornegger, William M. Wells, and Alejandro F. Frangi, editors, *Medical Image Computing and Computer-Assisted Intervention – MICCAI 2015*, pages 234–241, Cham, 2015. Springer International Publishing.
- [77] Angela Fan, Mike Lewis, and Yann Dauphin. Hierarchical neural story generation. In Iryna Gurevych and Yusuke Miyao, editors, *Proceedings of the 56th Annual Meeting of the Association for Computational Linguistics (Volume 1: Long Papers)*, pages 889–898, Melbourne, Australia, July 2018. Association for Computational Linguistics.
- [78] Alexander Quinn Nichol and Prafulla Dhariwal. Improved denoising diffusion probabilistic models. In *International Conference on Machine Learning (ICML)*, pages 8162–8171. PMLR, 2021.
- [79] Emiel Hoogeboom, Jonathan Heek, and Tim Salimans. simple diffusion: End-to-end diffusion for high resolution images. In *International Conference on Machine Learning (ICML)*, pages 13213–13232. PMLR, 2023.
- [80] Kyuhong Shim, Wonyong Sung, et al. Understanding the role of self attention for efficient speech recognition. In *International Conference on Learning Representations (ICLR)*, pages 1–19. International Conference on Learning Representations, ICLR, 2022.

8 Appendix

8.1 Dataset Details

English We use the following datasets: 1) Multilingual LibriSpeech (MLS) [61], which comprises transcribed speech from multiple speakers and languages, sourced from LibriVox audiobooks. 2) GigaSpeech [62], containing multi-domain speeches, such as audiobooks, podcasts, and YouTube videos, with human transcriptions. This dataset includes audio from multiple speakers but lacks speaker information. 3) LibriTTS-R [63], a restored version of the LibriTTS [64] corpus, sharing the same metadata. 4) VCTK [65] and 5) LJSpeech [66], which are widely used English datasets in the speech synthesis community, with VCTK being multi-speaker and LJSpeech being single-speaker. Additionally, we include the 6) Espresso Dataset [67] in DiTTo-en training. This high-quality (48,000 Hz) expressive speech collection features read speech and improvised dialogues from four speakers, totaling 40 hours.

We train a speech length predictor for DiTTo-en using the same datasets, but also include the LibriSpeech [53] dataset. This is due to the dependency on text normalization. MLS datasets consist of audio recordings, each ranging from about 10 to 20 seconds in length, paired with normalized text. It affects the speech length predictor, making it output lengths based on whether the input text is normalized. For example, if we input normalized text, the model tends to predict its speech length in the same range as MLS. While the text in LibriSpeech is also normalized, it offers more varied speech lengths, thus reducing the dependency on text normalization when determining speech lengths.

Korean We use the following datasets: 1) AIHub 14⁴, which features recordings of everyday people reading provided script sentences. 2) AIHub 15⁵, which has recordings of 50 professional voice actors expressing seven emotions (joy, surprised, sad, angry, scared, hate, neutral), five speaking styles (narrating, reading, news-like, dialogic, broadcasting), and three vocal ages (kid, young, old). 3) KsponSpeech [68], which consists of 2,000 speakers, each recording individual free speech on various topics in a quiet environment. The transcription follows specific guidelines regarding laughter, breathing, and more. 4) AIHub-broadcast⁶, which is designed for speech recognition and includes 10,000 hours of multi-speaker conversations recorded at 16,000 Hz, covering a wide range of 22 categories without annotations for speaker identity or emotional state. We also include 5) AIHub-expressive⁷, a dataset designed for speech synthesis, comprising 1,000 hours of speech recorded at 44,100 Hz. This dataset features 89 speakers and includes 7 speech styles (monologue, dialogue, storytelling, broadcast, friendly, animation, and reading) and 4 emotional tones (happiness, sadness, anger, and neutral).

Other Language We use subsets of MLS including German, Dutch, French, Spanish, Italian, Portuguese, and Polish.

Dataset Preprocessing Audio stream and its metadata are preprocessed and stored into parquet format. This allows fetching data with minimal IO-overhead from Network Attached Storage, allowing faster training. Parquets consisting of 10K pairs of audio and its metadata are compressed into TAR format, which further compresses to minimize data read overhead. While training, TAR files are decompressed, and parquets are deserialized into audio streams and its corresponding metadata in json format.

8.2 Experimental Setup Details

For English-only evaluations, we transcript generated audio using the CTC-based HuBERT-Large model⁸ [69]. For Multilingual Evaluations, we utilize OpenAI’s Whisper model⁹ [70]. Text nor-

⁴<https://www.aihub.or.kr/aihubdata/data/view.do?currMenu=115&topMenu=100&aihubDataSe=realm&dataSetSn=542>

⁵<https://www.aihub.or.kr/aihubdata/data/view.do?currMenu=115&topMenu=100&aihubDataSe=realm&dataSetSn=466>

⁶<https://www.aihub.or.kr/aihubdata/data/view.do?currMenu=115&topMenu=100&aihubDataSe=realm&dataSetSn=463>

⁷<https://www.aihub.or.kr/aihubdata/data/view.do?currMenu=115&topMenu=100&aihubDataSe=realm&dataSetSn=71349>

⁸<https://huggingface.co/facebook/hubert-large-ls960-ft>

⁹<https://github.com/openai/whisper/blob/main/model-card.md>: "large-v2"

malization is conducted using NVIDIA’s NeMo-text-processing¹⁰ [71, 72]. In both evaluations, WavLM-TDCNN¹¹ [73] is employed to evaluate SIM-o and SIM-r [31].

We conduct subjective evaluations using Amazon Mechanical Turk (MTurk) with US-based evaluators. For SMOS, evaluators assess the likeness of samples to the provided speech prompts, considering speaker similarity, style, acoustics, and background disturbances. In CMOS, evaluators compare the overall quality of a synthesized sample to a reference. They use a given scale to judge whether the synthesized version is superior or inferior to the reference. SMOS employs a 1 to 5 integer scale, where 5 signifies top quality. CMOS uses a scale from -3 (indicating the synthesized speech is much worse than the reference) to 3 (indicating it’s much better), with 1-unit intervals. Samples receive 6 and 12 ratings for SMOS and CMOS, respectively.

8.3 Baseline Details

The followings are the details of the baselines we used to compare with our model:

- VALL-E [25]: A zero-shot TTS model integrates autoregressive and non-autoregressive models. We show the objective metric scores directly extracted from the paper. We also present subjective evaluation results by comparing our samples with demo samples, which are at sample rates of 22,050 Hz and 16,000 Hz, respectively.
- SPEAR-TTS [27]: A multi-speaker TTS model that treats TTS as a two-step sequence-to-sequence process. It first converts text into high-level semantic tokens, similar to "reading," and then transforms these semantic tokens into low-level acoustic tokens, akin to "speaking." We present the objective metric scores directly from the paper.
- CLaM-TTS [15]: An advanced neural codec language model that uses probabilistic residual vector quantization to compress token length, enabling the simultaneous generation of multiple tokens, in contrast to VALL-E’s cascaded modeling approach. We offer both objective and subjective comparisons between our samples and those generated from the official model checkpoints.
- YourTTS [58]: A conventional TTS model based on the VITS [74] framework for zero-shot multi-speaker and multilingual training. We show both objective and subjective comparisons between our samples and those generated from the model checkpoints. We use the official checkpoint¹².
- VoiceBox [31]: A generative model employs a non-autoregressive flow-based architecture to tackle TTS as a text-guided speech infilling task, utilizing a large dataset. We present the objective metric scores directly from the paper. Additionally, we provide subjective evaluation results by comparing our samples with demo samples, recorded at sample rates of 22,050 Hz and 16,000 Hz, respectively.
- Simple-TTS [13]: A Latent Diffusion Model (LDM) based on U-ViT [60] serves as an alternative to complex TTS synthesis pipelines, removing the need for phonemizers, forced aligners, or detailed multi-stage processes. We provide both objective and subjective comparisons between our samples and those generated from the model checkpoints. We use the official checkpoint¹³.
- NaturalSpeech 2 [12]: A non-autoregressive TTS system that incorporates a neural audio codec employing residual vector quantizers to obtain quantized latent vectors. These vectors serve as input for a diffusion model, which generates continuous latent vectors conditioned on text input. Additionally, the system employs a speech prompting mechanism along with duration and pitch predictors. We present subjective evaluation results by comparing our samples with demo samples, which are at sample rates of 22,050 Hz and 16,000 Hz, respectively.
- NaturalSpeech 3 [33]: A non-autoregressive TTS system with factorized diffusion models based on a factorized vector quantization (FVQ) to disentangle speech waveforms into

¹⁰<https://github.com/NVIDIA/NeMo-text-processing>

¹¹https://github.com/microsoft/UniSpeech/tree/main/downstreams/speaker_verification

¹²<https://github.com/Edresson/YourTTS>

¹³<https://github.com/asappresearch/simple-tts>

Table 6: d_c is the embedding dimension of pretrained encoder, and d_h is the hidden dimension of DiTTo. SiLU is used as activation function between two linear layers.

Configuration	Num Layers	Input Dim	Hidden Dim	Out Dim
Timestep Embedder	2	256	d_h	d_h
Text Embedder	2	d_c	d_h	d_h
Skip Block	2	$2 \times d_h$	d_h	d_h
Final MLP	2	d_c	d_h	d_h
AdaLN Modulation	1	d_h	-	$9 \times d_h$

distinct subspaces such as content, prosody, timbre, and acoustic details. We present subjective evaluation results by comparing our samples with demo samples, which are at sample rates of 22,050 Hz and 16,000 Hz, respectively.

- Mega-TTS [59]: A TTS system that decomposes speech into attributes like content, timbre, prosody, and phase, with each attribute modeled by a module using appropriate inductive biases. We show subjective evaluation results by comparing our samples with demo samples, which have sample rates of 22,050 Hz and 16,000 Hz, respectively.
- E3-TTS [14]: A simple and efficient diffusion based TTS model which takes plain text as input. Unlike previous work, it doesn't rely on intermediary representations like spectrogram features or alignment data. We present subjective evaluation results by comparing our samples with demo samples, which are at sample rates of 22,050 Hz and 24,000 Hz, respectively.

8.4 Model Configuration

Table 7: Model parameters across different versions of DiTTo

Configuration	DiTTo-S	DiTTo-B	DiTTo-L	DiTTo-XL
Num Layers	12	12	24	28
Hidden Dim (d_h)	384	768	1024	1152
Num Heads	6	12	16	16

Our architecture is based on DiT [10] with several modifications. We extract text embeddings from a pre-trained text encoder, either from speechT5 [54] or ByT5 [55], and use these embeddings as hidden states in cross-attention layers. Adaptive layer normalization (AdaLN) layers condition on both time and text embeddings. AdaLN outputs modulate the layers within each transformer block. We apply RoPE [51] in self-attention layers. Following [9], we use a single global-AdaLN, sharing AdaLN parameters across all layers instead of using separate AdaLN for each layer. The global AdaLN layer conditions on both time and text, which are embedded and transformed with MLP layers. AdaLN generates scaling, shifting, and gating vectors for each self-attention, cross-attention, and MLP layer. Gating vectors modulate the outputs of each layer over the skip connections in transformer blocks. The vectors generated by AdaLN are further shifted with layer-independent learnable vectors. The MLP block in each transformer block adopts the gating mechanism from [75], which is used in the first linear layer of the MLP block. Inspired by [60], we insert a long skip connection from the input to the output of the last transformer block, differing from [60], where U-Net-like [76] long skip connections are used between transformer blocks at opposing ends. The detailed configurations are shown in Table 6, and the parameters for the four different model sizes are listed in Table 7.

8.5 Training and Inference of Speech Length Predictor

Training We train two speech length predictors for DiTTo-en and DiTTo-multi. Each was trained using the same text encoder as the respective DiTTo models. Essentially, we followed the same configuration as mentioned above, but without gradient accumulation and with a maximum token size of 10,240 for 600K steps. The number of trainable parameters for the speech length predictors

is 33.18M for DiTTo-en and 33.58M for DiTTo-multi. Figure 4 presents a visualization of length sampling during training.

Inference After training the speech length predictor, we can perform inference by either calculating the expected value over all possible length values using its softmax logits or by sampling from a multinomial distribution based on the softmax logits. In both cases, we apply top- k sampling [77] with $K = 20$. For human subjective evaluation, we set the expected length of the test samples.

8.6 Noise Schedule and Classifier-Free Guidance

Noise Scheduler We use the cosine noise schedule [78] with scale-shift [13, 79]. Since the impact of noise schedules can vary depending on the resolution of the input, it may be necessary to shift the schedule to appropriately add noise across time steps. As discussed in Section 6.2, we test five different values of scale-shift and visualize them in Figure 5.

Classifier-Free Guidance To leverage classifier-free guidance [36] for its efficacy in diffusion-based generative modeling, we train both a conditional and an unconditional diffusion model simultaneously. This is achieved by omitting the text input with a probability of $p = 0.1$. In the cross-attention layers of DiTTo, we concatenate a learnable null embedding with the text features along the sequence dimension, following the approach of [13]. We eliminate the conditioning information by masking out the text embeddings during the cross-attention computation and setting the mean-pooled text embedding to zero.

8.7 Mel-VAE++

When Mel-VAE is finetuned with the guidance of a pre-trained language model, consistent improvement in performance is observed, closing the gap with the SpeechT5 encoder, which is trained on both unsupervised speech and language data. To improve our understanding of semantic content injection, we finetune Mel-VAE with various pre-trained text and speech encoder models. As shown in Table 8, the experiments use various combinations of DiTTo text encoders and Mel-VAE text encoders. When SpeechT5 is utilized as the text encoder for DiTTo, semantic content injection enhances the performance metrics; however, its gains, while positive, are not as substantial as those observed in the control, which is trained the same number of steps without auxiliary signal, denoted as '-'. When ByT5-base is used as the DiTTo text encoder, using ByT5-base as Mel-VAE semantic content injection model significantly boosts metrics. We additionally observe that HuBERT feature

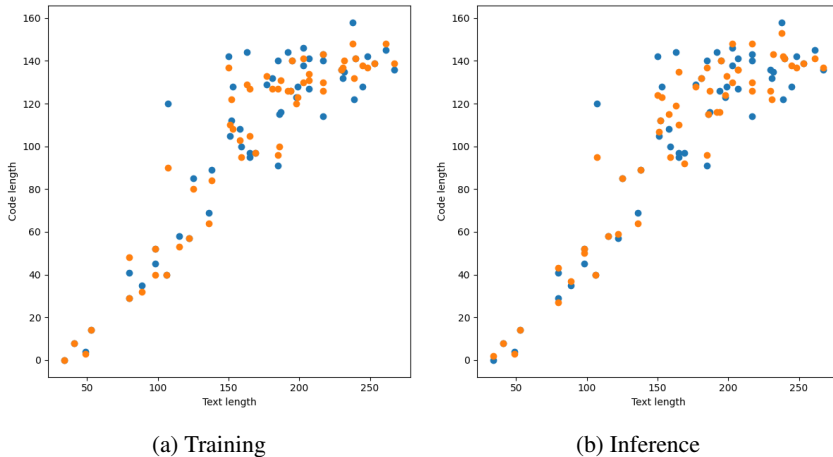


Figure 4: Visualization of outputs with the text input and approximately 3 seconds of speech prompt from the speech length predictor during (a) training and (b) inference. In both plots, the x -axis represents the length of text tokens, and the y -axis represents the length of speech tokens. The blue dots indicate the ground truth lengths of speech tokens for each text input, while the orange dots represent the lengths predicted by the speech length predictor.

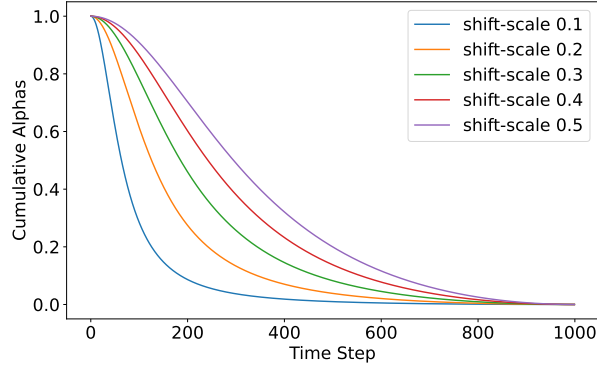
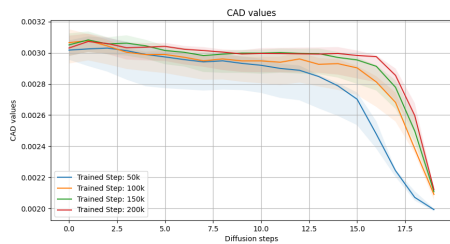


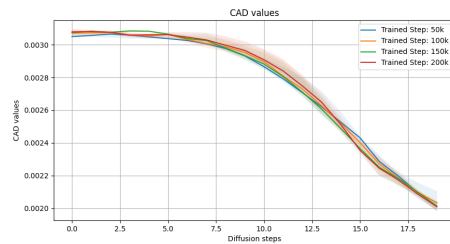
Figure 5: Visualization of our noise scheduler with various shift-scale factors. The x -axis represents the diffusion time steps, while the y -axis shows the cumulative alphas [1] of the noise scheduler.

Table 8: Performances of English-only cross-sentence task for Mel-VAE++. The boldface indicates the best result.

DiTTo Text Encoder	Mel-VAE++	WER ↓	CER ↓	SIM-o ↑	SIM-r ↑
SpeechT5	-	3.07	1.15	0.5423	0.5858
	HuBERT	5.59	3.18	0.5239	0.5742
	SpeechT5	3.09	1.12	0.5335	0.5940
	ByT5-base	2.99	1.06	0.5364	0.5982
	ByT5-base + HuBERT	2.93	1.04	0.5495	0.5958
ByT5-base	-	6.22	3.82	0.5482	0.5945
	HuBERT	5.88	3.64	0.5458	0.5938
	SpeechT5	4.10	1.95	0.5465	0.6055
	ByT5-base	3.11	1.17	0.5323	0.5965
	ByT5-base + HuBERT	3.69	1.72	0.5631	0.6101
ByT5-large	-	3.92	1.84	0.5292	0.5756
	HuBERT	3.04	1.11	0.5429	0.5878
	SpeechT5	3.27	1.31	0.5412	0.6029
	ByT5-base	3.17	1.18	0.5368	0.5999
	ByT5-base + HuBERT	3.80	1.75	0.5489	0.5975



(a) CAD without semantic injection



(b) CAD with semantic injection

Figure 6: Comparison of CAD between training with and without semantic injection

matching, as done in [44], helps refine its speech quality, as can be seen in the improved Speaker Similarity (SIM) metrics. When ByT5-base and HuBERT are both used, Mel-VAE benefits from both models.

We also investigate how DiTTo interacts with the text encoder latents as training progresses, in settings with and without semantic content injection. Since the TTS process typically ensures a monotonic alignment between text and speech, the diagonality of cross-attention between the text encoder and DiT block indicates how effectively text latents are used during denoising process. The intensity of the cross-attention map reflects how conducive the information provided by the text encoder is to producing DiTTo’s output. We measure the monotonicity of cross-attention maps using Cumulative Attention Diagonality (CAD) [80].

The median CAD values are drawn in solid lines as in Figure 6. The model performs inference on 5 samples. The Interquartile Range (IQR) is represented by the shaded regions surrounding the solid lines in the graph. We set the sampling steps as 25, noise schedule scale shift as 0.3, and classifier-free guidance scale as 5.0. Given that the parameters of text encoders are not tuned during DiTTo training, drastic changes in CAD values across training steps without semantic content injection indicate significant changes in DiTTo parameters are needed to align with text encoders. In contrast, with semantic content injection, changes in CAD values as training progresses show minimal fluctuation. This suggests that semantic content injection enables effective interaction between text encoders and DiT blocks. Based on CAD values across diffusion steps, semantic content injection allows the interaction between the text encoder and DiTTo to predominantly occur during the initial stages of the reverse process. This suggests that semantic content injection boosts the provision of rich semantic information by text encoders, allowing DiT blocks to focus on improving acoustic quality in later steps. Furthermore, the significant deviations across samples, as evidenced by the enlarged shaded regions when semantic injection is not employed, suggest that the interaction between the text encoder and DiT blocks is less effective without semantic content injection.

8.8 Human Evaluations on Comparison of Demo Samples

Table 9: Human evaluations on comparison of demo samples from various SOTA models with DiTTo-en (XL). SMOS scores include a 95% confidence interval. The boldface indicates the best result.

Model	SMOS	CMOS
Voicebox [31]	2.87±0.45	0.14
DiTTo-en	3.57±0.39	0.0
VALL-E [25]	3.50±0.46	-0.94
DiTTo-en	3.90±0.38	0.0
MegaTTS [59]	3.76±0.44	-0.31
DiTTo-en	3.82±0.32	0.0
E3-TTS [14]	4.25±0.19	-0.30
DiTTo-en	4.28±0.32	0.0
NaturalSpeech 2 [12]	3.99±0.37	-0.29
DiTTo-en	4.01±0.35	0.0
NaturalSpeech 3 [33]	4.42±0.28	-0.27
DiTTo-en	3.92±0.27	0.0

Table 9 shows the results of human evaluation on demo cases. DiTTo outperforms all others except for NaturalSpeech 3 in SMOS and Voicebox in CMOS. We hypothesize that the prompts used in Voicebox tends to be unintelligible and noisy, and as shown in SMOS, the model samples did not adhere to them well. In contrast, DiTTo follows the prompts better, although the naturalness of the samples themselves is somewhat lacking. Therefore, in CMOS, when comparing two samples without prompts, it is likely that DiTTo will be judged as less natural. Conversely, in NaturalSpeech 3, as shown in SMOS, the model follows the intonation of the prompts too closely, sometimes resulting in unnaturalness. Thus, when comparing samples without prompts, DiTTo may sound more natural.

8.9 Multilingual Continuation Task

In this section, we provide the experimental results of multilingual continual tasks for both DiTTo-multi in Table 10 and CLaM-multi in Table 11.

Table 10: Performances of DiTTo-multi for the multilingual *continuation* task.

Model	WER ↓	CER ↓	SIM-o ↑	SIM-r ↑
English / MLS English	6.91	4.15	0.4759	0.4986
English (HuBERT) / MLS English	5.73	1.84	-	-
German / MLS German	6.60	2.47	0.4917	0.5239
Dutch / MLS Dutch	8.89	3.11	0.5828	0.5971
French / MLS French	8.03	3.09	0.5711	0.5905
Spanish / MLS Spanish	2.22	0.89	0.5483	0.5776
Italian / MLS Italian	13.69	2.35	0.5637	0.5902
Portuguese / MLS Portuguese	6.07	2.11	0.5346	0.5289
Polish / MLS Polish	10.88	3.17	0.5090	0.5441
Korean / AIHub 14	19.44	1.90	0.5838	0.6095
Korean / AIHub 15	13.80	2.20	0.5260	0.5454
Korean / Ksponspeech	27.22	18.30	0.5205	0.5466

Table 11: Performances of CLaM-multi for the multilingual *continuation* task.

Model	WER ↓	CER ↓	SIM-o ↑
English / MLS English	8.71	5.19	0.4000
English (HuBERT) / MLS English	7.71	3.19	0.4000
German / MLS German	9.63	4.11	0.4219
Dutch / MLS Dutch	12.25	4.97	0.5983
French / MLS French	10.29	4.08	0.5671
Spanish / MLS Spanish	4.02	1.91	0.5292
Italian / MLS Italian	19.70	5.19	0.5459
Portuguese / MLS Portuguese	9.66	3.72	0.5658
Polish / MLS Polish	14.70	5.34	0.5519
Korean / AIHub 14	20.21	1.80	0.5423
Korean / AIHub 15	13.08	2.35	0.5280
Korean / Ksponspeech	30.24	20.02	0.4488